

预处理气氛对 $\text{CuO}/\text{CeO}_2/\gamma\text{-Al}_2\text{O}_3$ 催化剂表面性质及“NO+CO”反应性能的影响

朱 捷* 葛奉娟

(徐州工程学院化学化工学院, 徐州 221111)

摘要: 用不同的预处理气氛制备了 $\text{CeO}_2/\gamma\text{-Al}_2\text{O}_3$ 载体以调节表面 Ce 的价态, 并以 $\text{Cu}(\text{CH}_3\text{COO})_2$ 为前驱体制备了 CuCeAl 催化剂。XRD 和 H_2 -TPR 的结果表明在还原气氛下处理的 $\text{CeO}_2/\gamma\text{-Al}_2\text{O}_3$ 载体具有更多的活性氧原子, 因此相应的 CuCeAl 催化剂表面有更多分散态的 $\text{Cu}^{2+}/\text{Cu}^+$ 物种。NO+CO 反应的结果表明分散态的 $\text{Cu}^{2+}/\text{Cu}^+$ 是 NO 转化的活性物质, 而 Cu^0 在低温下具有较好的 N_2 选择性。因此, 同时含有分散态 $\text{Cu}^{2+}/\text{Cu}^+$ 和少量晶相 Cu^0 的催化剂具有最好的催化性能。

关键词: 多相催化; 氮氧化物; 污染防治; 预处理气氛; $\text{CeO}_2/\gamma\text{-Al}_2\text{O}_3$; “NO +CO”反应

中图分类号: O611.62 文献标识码: A 文章编号: 1001-4861(2015)01-0191-07

DOI: 10.11862/CJIC.2015.021

CuO/CeO₂/γ-Al₂O₃ Catalysts: Effect of Pretreating Atmosphere on Surface Properties and Catalytic Performance in Selective Catalytic Reduction of NO with CO

ZHU Jie* GE Feng-Juan

(School of Chemistry and Chemical Engineering, Xuzhou Institute of Technology, Xuzhou, Jiangsu 221111, China)

Abstract: The $\text{CeO}_2/\gamma\text{-Al}_2\text{O}_3$ supports were prepared and pretreated in different atmospheres to adjust the valence state of surface Ce element, then Cu (CH_3COO)₂ was impregnated as the precursor to prepare CuCeAl samples. XRD and H_2 -TPR results indicate that the $\text{CeO}_2/\gamma\text{-Al}_2\text{O}_3$ support pretreated by reducing atmosphere has more active oxygen atoms, consequently has more dispersed $\text{Cu}^{2+}/\text{Cu}^+$ species on the surface. The “NO+CO” reaction tests reveal that the dispersed $\text{Cu}^{2+}/\text{Cu}^+$ are the active species for NO conversion, while crystalline Cu^0 promotes the N_2 selectivity at low temperatures. Hence, the catalysts containing both dispersed $\text{Cu}^{2+}/\text{Cu}^+$ and a few crystalline Cu^0 have the optimal catalytic efficiency.

Key words: heterogeneous catalysis; nitrogen oxides; waste prevention; pretreating atmosphere; $\text{CeO}_2/\gamma\text{-Al}_2\text{O}_3$; “NO+CO” reaction

0 Introduction

NO is the major source of air pollution, for it has the ability to generate secondary contaminants through its interaction with other primary pollutants^[1]. Catalytic reduction of NO in the presence of CO is one of the most important reactions occurring in automotive

catalytic converters, where both reactants are undesirable pollutants^[2]. Supported noble metal catalysts have been considered as the most efficient catalysts for their responsible activity, good hydrothermal and resistance to impurities such as SO_2 ^[3]. However, the scarcity and the high cost have limited their application. Copper-containing catalysts show a

收稿日期: 2014-07-03。收修改稿日期: 2014-10-15。

江苏省高校自然科学基金(No.12KJD530002)资助项目。

*通讯联系人。E-mail: zhujie19@xzit.edu.cn

potential activity for the treatment of exhaust gas from automobiles and have been extensively investigated during the past decades^[2,4-5].

CeO₂ is an important support and has attracted more attention recently due to its outstanding oxygen storage capacity and unique redox properties^[6-8]. A number of reports have shown that the conversion between Ce(III) and Ce(IV) oxidation states is likely the key factor leading to the high mobility of lattice oxygen and providing activation centers in some redox reactions^[9-11]. In our work, the CeO₂/γ-Al₂O₃ supports were prepared and then pretreated in different atmospheres to adjust the valence state of surface Ce element, the surface states of CuCeAl samples were characterized by XRD and H₂-TPR and the catalytic activity for NO+CO reactions was evaluated. The effect of pretreating atmosphere was discussed on the surface property and the NO+CO activity of the catalysts.

1 Experimental

1.1 Sample Preparation

γ-Al₂O₃ was purchased from Fushun Petrochemical Institute (China) with BET surface area of 140 m²·g⁻¹ and was calcined at 700 °C for 5 h before use.

CeO₂/γ-Al₂O₃ samples were prepared by impregnating the γ-Al₂O₃ with an aqueous solution containing required amount of Ce(NO₃)₃. The impregnated sample was dried at 100 °C for 12 h and then divided into three parts and calcined at 500 °C for 2 h in various atmospheres, respectively: H₂-Ar mixture (7.3% H₂ by volume), N₂ (≥99.5% by volume) and O₂ (≥99.9% by volume), the sample was denoted correspondingly as CeAl-H₂, CeAl-N₂, CeAl-O₂. The Ce loading was 0.07 mmol/100m² γ-Al₂O₃.

The CuO/CeO₂/γ-Al₂O₃ samples were prepared by impregnating the CeO₂/γ-Al₂O₃ support above with an aqueous solution containing required amount of copper acetate, then dried at 100 °C for 12 h. The samples were all calcined in flowing N₂ (≥99.5% by volume) at 450 °C for 5 h. For simplicity, the resultant samples were denoted as xCuCeAl-H₂, xCuCeAl-N₂

and xCuCeAl-O₂, respectively, where x stands for the loading amount of copper acetate (mmol/100m² γ-Al₂O₃). For comparison, the xCuO/γ-Al₂O₃ sample was also prepared by the same method.

1.2 Characterization

X-ray diffraction (XRD) patterns were obtained with a Philips Xpert Pro diffractometer using Ni filtered Cu Kα radiation (λ=0.154 18 nm). The X-ray tube was operated at 40 kV and 40 mA.

BET surface area was measured by nitrogen adsorption at 77 K on a Micromeritics ASAP-2020 adsorption apparatus.

Temperature-programmed reduction (TPR) was carried out in a quartz U-tube reactor, and 100 mg sample was used for each measurement. Before reduction, the sample was pretreated in N₂ stream at 100 °C for 1 h and then cooled to room temperature. After that, a H₂-Ar mixture (7% H₂ by volume) was switched on and the temperature was increased linearly at a rate of 10 °C·min⁻¹. A thermal conductivity cell was used to detect the consumption of H₂ on stream.

The activities of the catalysts for NO+CO reaction were evaluated under steady state, involving a feed stream with a fixed composition, NO 3.33%, CO 6.67% and He 90% by volume as diluter. A quartz tube was employed as the reactor and the required quantity of catalysts (50 mg for each test) was used. The catalysts were pretreated in N₂ stream at 100 °C for 1 h and then heated to reaction temperature, after that, the mixed gases were switched on. The reactions were carried out at 300 °C with the same space velocity of 30 000 mL·g⁻¹·h⁻¹. Two columns and thermal conductivity detector (TCD) were used for the purpose of analyzing the products. Column A was a stainless steel (9.525 mm (Φ3)×1.75 m) Porapak Q for separating N₂O and CO₂, and Column B was a stainless steel (9.525mm(Φ3)×1.75 m) 13X molecular sieve (30~60 Mesh(250~595 μm)) for separating N₂, NO and CO.

2 Results and discussion

2.1 XRD

Fig.1 shows the XRD patterns of 0.3CuAl,

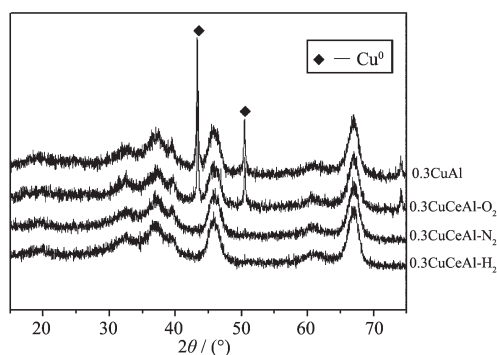


Fig.1 XRD patterns of 0.3CuAl and 0.3CuCeAl samples

0.3CuCeAl- O_2 , 0.3CuCeAl- N_2 and 0.3CuCeAl- H_2 samples. No crystalline peaks of ceria are observed for all Ce-modified samples, implying the possibility (albeit not complete proofing) of well dispersed CeO_2 on the surface of $\gamma\text{-Al}_2\text{O}_3$ ^[12-14]. For 0.3CuAl sample, characteristic peaks of Cu^0 metal are observed at 43° and 50° , indicating that there are many Cu^0 arising from the decomposition of $\text{Cu}(\text{CH}_3\text{COO})_2$. According to our previous results, the dispersion capacity of CuO on the surface of $\gamma\text{-Al}_2\text{O}_3$ is about 0.75 mmol/100m²^[15]. The result indicates that the Cu^0 species are difficult to disperse on the surface of $\gamma\text{-Al}_2\text{O}_3$ in our

experimental condition of $\text{Cu}(\text{CH}_3\text{COO})_2$ precursor and N_2 atmosphere.

The possible reasons should be as follows. According to the literatures^[16-18], for $\gamma\text{-Al}_2\text{O}_3$, the (110) plane is the preferentially exposed plane with the octahedral and tetrahedral vacancies, and this plane consists of C- and D-layers, which have equal exposure probabilities. When CuO are dispersed on the surface of $\gamma\text{-Al}_2\text{O}_3$, the Cu^{2+} cations incorporate into the octahedral vacant sites. Meanwhile, the capping oxygen atoms cover the Cu^{2+} to balance the charge, forming steady octahedral structures, as shown by Figures 2a and 2b. The average density of the octahedral vacant sites is 2 sites/unit mesh (0.443 5 nm², while 0.14 nm is taken as the radius of O^{2-} anion) of the C- and D-layers, corresponding to 0.75 mmol/100 m² $\gamma\text{-Al}_2\text{O}_3$. Thus, the theoretical dispersion capacity of CuO is 0.75 mmol/100 m² $\gamma\text{-Al}_2\text{O}_3$. When $\gamma\text{-Al}_2\text{O}_3$ is impregnated by $\text{Cu}(\text{CH}_3\text{COO})_2$ aqueous solution, Cu^{2+} cations will occupy the octahedral vacant sites on the surface of $\gamma\text{-Al}_2\text{O}_3$ and the two accompanying CH_3COO^- anions would stay at the top

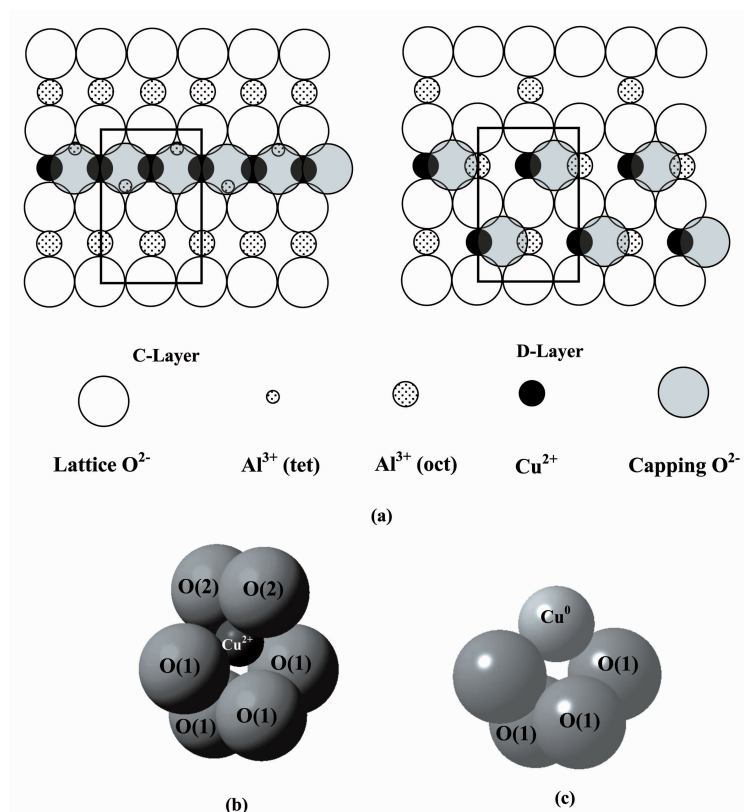


Fig.2 Scheme for $\text{Cu}^{2+}/\text{Cu}^0$ species dispersion on the surface of $\gamma\text{-Al}_2\text{O}_3$. O(1): surface oxygen, O(2): capping oxygen.

of the occupied site as capping anions, compensating the extra positive charges. Thus, the repulsion between acetate anions may hinder the dispersion of Cu^{2+} into the adjacent vacant sites of the $\gamma\text{-Al}_2\text{O}_3$, leading to the decrease of dispersion capacity. Another possible reason is that the decomposition gas of $\text{Cu}(\text{CH}_3\text{COO})_2$ is reductive and the calcination atmosphere is N_2 , thus the Cu^0 metal is the main decomposition product. The radius of Cu^0 atom is about 117 pm, while the radius of octahedral vacant sites is only 58 pm. Thus, Cu^0 is too large to incorporate steadily into the surface vacant sites, as shown in Fig. 2c. Furthermore, as Cu^0 metal has no positive charges, the absence of electrostatic attraction makes it difficult to disperse.

However, it is noteworthy that, for 0.3CuCeAl- N_2 and 0.3CuCeAl- H_2 , no any crystalline peaks of Cu species could be observed. As analyzed before, Cu^0 can hardly incorporate into the surface vacant sites of $\gamma\text{-Al}_2\text{O}_3$. Thus, CeO_2 should promote the production of Cu species with higher valence states, i.e., Cu^+ or Cu^{2+} , in the 0.3CuCeAl- N_2 and 0.3CuCeAl- H_2 samples. While for 0.3CuCeAl- O_2 , the crystalline peaks of Cu^0 metal could be observed obviously and the peak intensity is comparative with that in 0.3CuAl sample, implying that the CeO_2 in 0.3CuCeAl- O_2 sample has little effect on the valence states of Cu species and most of Cu species are still crystalline Cu^0 metal. The result indicates that the calcination atmosphere of CeAl support is very important for its surface structure and properties.

The difference between 0.3CuCeAl- N_2 , 0.3CuCeAl- H_2 and 0.3CuCeAl- O_2 can be explained by the oxygen deficiency property of CeO_2 . As Ce content is very few ($0.07 \text{ mmol}/100\text{m}^2 \gamma\text{-Al}_2\text{O}_3$), it is reasonable to assume that the Cu species are dispersed on the surface of $\gamma\text{-Al}_2\text{O}_3$. CeO_2 is actually a nonstoichiometric compound, i.e., CeO_{2-x} , where oxygen vacant sites are considered to be present in the lattice in a randomized fashion^[19]. As oxygen deficiency can improve the mobility of oxygen atoms in the lattice, the modified ceria could provide active oxidation sites on the surface of CeAl support. In the calcination

process of CeAl supported Cu $(\text{CH}_3\text{COO})_2$, the active oxygen atoms of ceria react with adjacent Cu atoms and produce Cu^+ or Cu^{2+} species, which can incorporate into the octahedral vacant sites of $\gamma\text{-Al}_2\text{O}_3$. While for 0.3CuCeAl- O_2 , as CeAl- O_2 support is calcined in O_2 atmosphere, the CeO_2 is oxidized greatly and the oxygen deficiency decreases sharply, which lowers the oxygen mobility significantly. Thus, the Cu species mainly exist as Cu^0 metal, which could not disperse effectively on the surface of $\gamma\text{-Al}_2\text{O}_3$.

2.2 H_2 -TPR

For comparison of the amount of dispersed Cu species further, H_2 -TPR was performed for CuAl and CuCeAl samples and the results are shown in Fig.3. A reduction peak at about 210 °C appears in all samples, corresponding to the reduction of CuO_x dispersed on $\gamma\text{-Al}_2\text{O}_3$. As the reduction temperature of Cu species for CeO_2 modified samples are very close to CuAl sample and the reduction temperature of dispersed CuO on CeO_2 support is 150~180 °C^[20], it can be concluded that the Cu species disperse on the surface of $\gamma\text{-Al}_2\text{O}_3$ and CeO_2 has little promotion effect on the reduction of Cu species in our samples. For CuCeAl- O_2 , another peak at about 232 °C can be observed. According to the literatures^[21-22], the reduction of absorbed oxygen on the surface of ceria are about 226 and 268 °C, so we attribute it here to the reduction of absorbed oxygen molecules on the surface of CeO_2 , which are absorbed during the pretreatment in oxygen atmosphere.

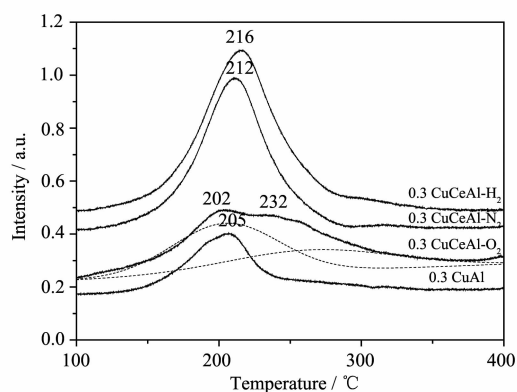


Fig.3 TPR profiles of supported Cu catalysts.
(a) 0.3CuAl (b) 0.3CuCeAl- O_2 (c)
0.3CuCeAl- N_2 and (d) 0.3CuCeAl- H_2

The peak areas of the CuCeAl samples are different with the calcination atmosphere as shown in Fig.3. The peak areas for CuO_x reduction of 0.3CuAl, 0.3CuCeAl-O₂, 0.3CuCeAl-N₂ and 0.3CuCeAl-H₂ are 14.5, 12.1, 35.1 and 42.2, respectively, which are ordered as: 0.3CuCeAl-H₂ > 0.3CuCeAl-N₂ >> 0.3CuCeAl-O₂ ≈ 0.3CuAl. It should be noted that the H₂ consumption of 0.3CuCeAl-H₂ is about 20% larger than 0.3CuCeAl-N₂, indicating that 0.3CuCeAl-H₂ has more Cu²⁺ than 0.3CuCeAl-N₂. The reason should be that CeAl-H₂ support pretreated in reductive atmosphere has more oxygen vacancies at the surface and therefore has more active oxygen atoms. For CuCeAl-O₂, the area of CuO reduction peak is very weak, as well as 0.3CuAl, indicating that the CeAl-O₂ sample has very little oxygen deficiencies and poor oxygen mobility, thus has no promotion effect on the formation of Cu²⁺/Cu⁺.

2.3 Catalytic activity and selectivity of NO reduction by CO

Fig.4 is the activity and selectivity results of NO+CO reaction for 0.3CuAl and 0.3CuCeAl samples. The NO conversion displays the following order: 0.3CuCeAl-H₂ > 0.3CuCeAl-N₂ > 0.3CuCeAl-O₂ > 0.3CuAl, which is positively correlated with the content of Cu²⁺/Cu⁺, implying that the dispersed Cu²⁺ facilitates the conversion of NO. The N₂ selectivity at lower temperature (≤250 °C) for 0.3CuCeAl-H₂ and 0.3CuCeAl-N₂ is very low, while that of 0.3CuAl is as high as about 80% as seen from the N₂ selectivity results (Fig.4b), and interestingly, the N₂ selectivity of 0.3CuCeAl-O₂ sample is just between the above two. The results indicate that 0.3CuCeAl-H₂ and

0.3CuCeAl-N₂ convert NO mostly into N₂O. It should be noted that the N₂ selectivity is in accordance with the content of crystalline Cu⁰ metal. Therefore, it can be concluded that the crystalline Cu⁰ metal is the active species for N₂ selectivity, i.e., the Cu⁰ promotes the conversion of N₂O to N₂^[23].

To further investigate the effects of the state of copper species on the activity and selectivity of “NO+CO” reaction, 0.6CuCeAl-H₂ and 0.6CuAl samples were prepared and their XRD and H₂-TPR results are shown in Fig.5. From XRD result (Fig.5a), the diffraction peaks of crystalline Cu⁰ metal for 0.6CuCeAl-H₂ sample appear when the Cu loading increases to 0.6 mmol/100m², indicating that the modified CeO₂ with loading of 0.07 mmol/100 m² is not enough to oxidize all Cu⁰ species. Thus, some crystalline Cu⁰ remains in the sample. Furthermore, the H₂-TPR result (Fig.5b) shows that the peak area of 0.6CuCeAl-H₂ is much larger than that of 0.6CuAl, also indicating that 0.6CuCeAl-H₂ contains much more Cu²⁺/Cu⁺ than 0.6CuAl.

Figures 5c and 5d are the activity results of NO+CO reaction for CuCeAl-H₂ and CuAl samples. The NO conversion of CuCeAl-H₂ is obviously higher than corresponding CuAl samples as shown in Fig.5c, which further proves that the Cu²⁺/Cu⁺ species are the active species for NO reduction by CO. In addition, 0.6CuCeAl-H₂ has much higher NO conversion activity than that of 0.3CuCeAl-H₂. The NO turn-over frequency (TOF) of each copper ion (i.e. the NO turn-over number of each copper ion at 250 °C per hour) is presented in Table 1. 0.6CuCeAl-H₂ still keeps relatively higher TOF. Meanwhile, as Fig.5d shows,

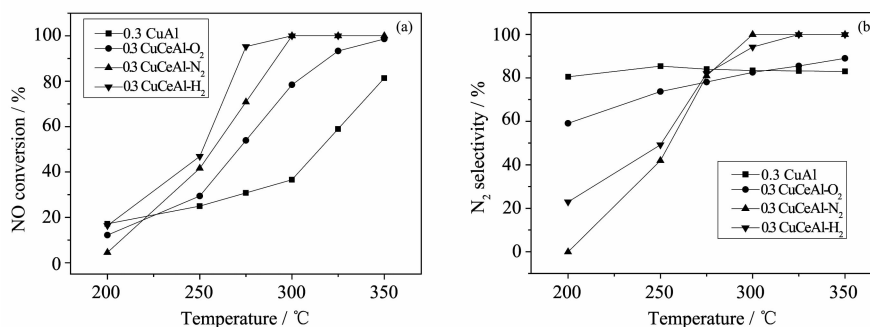


Fig.4 NO conversion (a) and N₂ selectivity (b) of 0.3CuAl and 0.3CuCeAl samples for “NO+CO” reaction

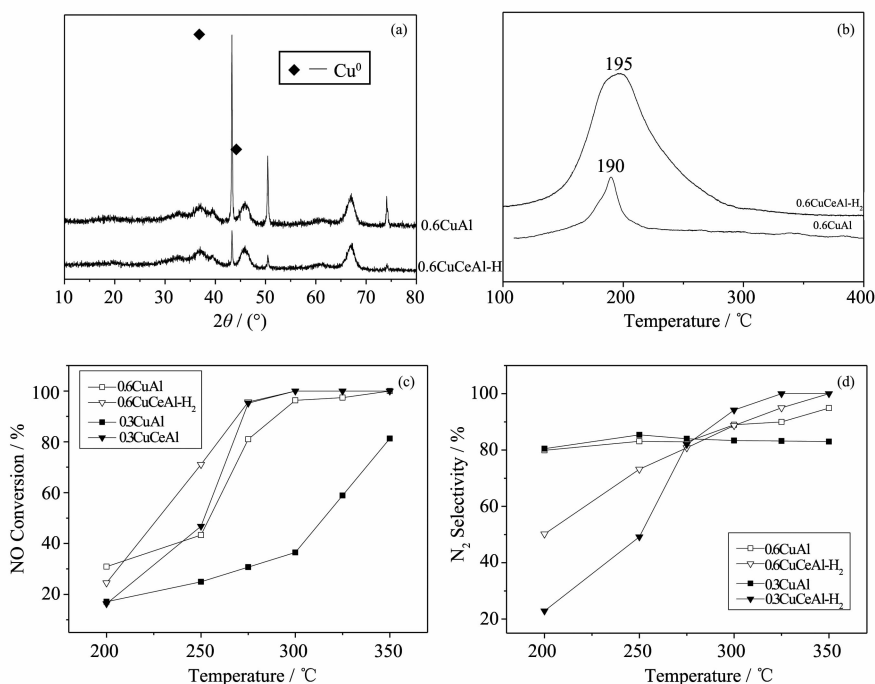


Fig.5 (a) XRD patterns of 0.6CuAl and 0.6CuCeAl-H_2 ; (b) H_2 -TPR of 0.6CuAl and 0.6CuCeAl-H_2 ; NO conversion (c) and N_2 selectivity (d) of some CuAl and CuCeAl samples for “NO+CO” reaction

Table 1 NO TOF and N_2 TOF for NO+CO reaction of some CuAl and CuCeAl sample

	0.3CuAl	0.3CuCeAl-H ₂	0.6CuAl	0.6CuCeAl-H ₂
NO TOF	24.3	45.6	21.1	34.6
N_2 TOF	20.8	22.4	17.5	25.3

both CuAl samples have rather high N_2 selectivity in low temperatures. The N_2 selectivity of 0.6CuCeAl-H_2 also increases obviously compared with 0.3CuCeAl-H_2 , indicating that the crystalline Cu^0 metal is the key species for low-temperature N_2 selectivity. Comparing the N_2 TOF at 250 $^{\circ}\text{C}$ ($\text{N}_2\text{TOF}=(\text{NO TOF}) \cdot (\text{N}_2 \text{ selectivity})$) (Table 1), it can be concluded that 0.6CuCeAl-H_2 has higher catalytic efficiency.

3 Conclusions

The $\text{CeO}_2/\gamma\text{-Al}_2\text{O}_3$ supports have been pretreated in different atmospheres. The surface states suggest that the $\text{CeO}_2/\gamma\text{-Al}_2\text{O}_3$ support pretreated by reducing atmosphere has more surface oxygen vacancies, consequently has more active oxygen atoms. Therefore, the CuCeAl-H₂ has more dispersed Cu^{2+} on the surface. NO+CO activity results reveal that dispersed $\text{Cu}^{2+}/\text{Cu}^+$ is the active species for NO conversion, while

crystalline Cu^0 metal promotes the N_2 selectivity at low temperatures, i.e., facilitates the conversion of N_2O to N_2 . Hence, the catalysts containing both dispersed CuO and a few crystalline Cu^0 species have the best catalytic efficiency.

Acknowledgements: The financial support of General Project of University Science Research of Jiangsu Province (12KJD530002) is gratefully acknowledged. Li Lulu in School of Chemistry, Nanjing University is also gratefully acknowledged for generous technical assistance.

References:

- [1] Schneider H, Scharf U, Baiker A, et al. *J. Catal.*, **1994**,**146**: 545-556
- [2] Parvulescu V, Grange P, Delmon B. *Catal. Today*, **1998**,**46**: 233-316
- [3] Guimaraes A, Dieguez L, Schmal M. *J. Phys. Chem. B*,

- 2003,107**:4311-4319
- [4] Shan W J, Shen W J, Li C. *Chem. Mater.*, **2003,15**:4761-4767
- [5] Zhu H Y, Shen M M, Gao F, et al. *Catal. Commun.*, **2004,5**:453-456
- [6] Hennings U, Reimert R. *Appl. Catal. A: Gen.*, **2007,325**:41-49
- [7] Bernal S, Blanco G, Pintado J, et al. *Catal. Commun.*, **2005,6**:582-585
- [8] Liang Q, Wu X D, Weng D, et al. *Catal. Commun.*, **2008,9**:202-206
- [9] Qi G, Yang R T. *J. Catal.*, **2003,217**:434-441
- [10] Dyakonov A J, Little C A. *Appl. Catal. B: Environ.*, **2006,67**:52-59
- [11] He H, Dai H X, Wong K W. *Appl. Catal. A: Gen.*, **2003,251**:61-74
- [12] Hu Y, Dong L, Wang J, et al. *J. Mol. Catal. A*, **2000,162**:307-316
- [13] Stranick M A, Houalla M, Hercules D M. *J. Catal.*, **1987,106**:362-368
- [14] Chen Y, Dong L, Jin Y S, et al. *Stud. Surf. Sci. Catal.*, **1996,101**:1293-1302
- [15] Xia W S, Wan H L, Chen Y. *J. Mol. Catal. A: Chem.*, **1999,138**:185-195
- [16] Schuit G A, Gates B C. *AIChE J.*, **1973,19**:417-438
- [17] Chen Y, Zhang L F. *Catal. Lett.*, **1992,12**:51-62
- [18] Jimenez-Gonzalez J, Schmeisser D. *Surf. Sci.*, **1991,250**:59-70
- [19] Trovarelli A. *Catalysis by Ceria and Related Materials*. Singapore: World Scientific, **2013**.
- [20] Zou H B, Dong X F, Lin W M. *Appl. Surf. Sci.*, **2006,253**:2893-2898
- [21] Li Y, Zhang B C, Tang X L, et al. *Catal. Commun.*, **2006,7**:380-386
- [22] Zhu Jie, Gao Fei, Dong Li-Hui, et al. *Appl. Catal. B: Environ.*, **2010,95**:144-152
- [23] Sagar G V, Rao P V R, Srikanth C S, et al. *J. Phys. Chem. B*, **2006,110**:13881-13888